

Comparative Study of the High-Pressure Behavior of As, Sb, and Bi

Ulrich Häussermann,* Karin Söderberg,[†] and Rolf Norrestam[†]

Contribution from the Department of Inorganic Chemistry, Stockholm University,
S-10691 Stockholm, Sweden

Received June 11, 2002. Revised Manuscript Received September 25, 2002

Abstract: The high-pressure behavior of the heavier group 15 elements As, Sb, and Bi was investigated by means of ab initio density functional calculations employing pseudopotentials and a plane wave basis set. The high-pressure structural sequence of these elements is distinguished by the occurrence of the Bi-III structure, which is a complex, incommensurately modulated, host–guest structure. We approximated this structure by a supercell which reproduced the experimentally established pressure stability ranges of the host–guest structure for the different elements extremely well. With pressure we find an increasing admixture of d states (s–d hybridization) in the occupied levels of the electronic structure of As, Sb, and Bi. However, the s–d mixing remains at a low level. Thus, the emergence of a complex intermediate pressure structure cannot be explained by a pressure-induced altered valence state for these elements. Instead, it is argued that the Bi-III structure is a consequence of a delicate interplay between the electrostatic and the band energy contribution to the total energy. In the intermediate pressure range of heavier group 15 elements, both important parts of the total energy account equally for structural stability.

1. Introduction

High-pressure experiments allow the study of structural stability as a function of volume. This possibility has added a new dimension to the fundamental question concerning the relation between atom arrangement and electronic structure. In this respect, recent high-pressure investigations of main group elements have yielded many surprising and intriguing results. For example, it was found that with pressure several alkali metal and alkaline earth metals violate the pressure–coordination rule and transform from simple densely packed to more open packed structures.^{1–5} Moreover, these high-pressure structures can attain a remarkable complexity, which culminated in the discovery that the structures of Ba-IV and Sr-V correspond to self-hosting incommensurate assemblies.^{6,7}

The occurrence of a host–guest structure in an element, where the host and guest are formed by the same component, is most unusual and has attracted much attention.⁸ The structures of Ba-IV and Sr-V, which are stable over a wide range of pressures, represent not just a curiosity. Recently, it was found that high-

pressure phases of Rb (Rb-IV),⁹ Bi, and Sb (Bi-III and Sb-II, respectively)¹⁰ also adopt an incommensurate host–guest structure. Interestingly, the arrangement of the host atoms in the group 15 element modifications Bi-III and Sb-II corresponds to that of the alkaline earth metals Ba-IV and Sr-V. Thus, elemental high-pressure modifications with host–guest structures may be rather frequent and the reason behind this new phenomenon is not yet understood.

In this article we report our investigations into the high-pressure behavior of the heavier group 15 elements As, Sb, and Bi by means of ab initio calculations employing pseudopotentials and a plane wave basis set. In particular, by this comparative study we aim to elucidate the origin of the (incommensurate) host–guest structure in the high-pressure structural sequence of As, Sb, and Bi, and we attempt to establish general electronic structure trends for these elements under compression. This covers also the interesting aspect of the semimetal–metal transition of the group 15 elements under moderate compression. However, since this issue has already been the subject of a number of previous works,^{11–15} it is only briefly addressed in this paper.

2. Computational Details

Total energy calculations for As, Sb, and Bi as a function of volume were performed within ab initio density functional theory using

* Corresponding author. E-mail: ulrich@inorg.su.se.

[†] Department of Structural Chemistry, Stockholm University, S-10691 Stockholm, Sweden.

- (1) Hanfland, M.; Syassen, K.; Christensen, N. E.; Novikov, D. L. *Nature* **2000**, *408*, 174.
- (2) Schwarz, U.; Grzechnik, A.; Syassen, K.; Hanfland, M. *Phys. Rev. Lett.* **1999**, *83*, 4085.
- (3) Schwarz, U.; Takemura, K.; Hanfland, M.; Syassen, K. *Phys. Rev. Lett.* **1998**, *81*, 2711.
- (4) Olijnyk, H.; Holzappel, W. B. *Phys. Lett. A* **1984**, *100A*, 191.
- (5) Allan, D. R.; Nelmes, R. J.; McMahon, M. I.; Belmonte, S. A.; Bovornratanaraks, T. *Rev. High Pressure Sci. Technol.* **1998**, *7*, 236.
- (6) Nelmes, R. J.; Allan, D. R.; McMahon, M. I.; Belmonte, S. A. *Phys. Rev. Lett.* **1999**, *83*, 4081.
- (7) McMahon, M. I.; Bovornratanaraks, T.; Allan, D. R.; Belmonte, S. A.; Nelmes, R. J. *Phys. Rev. B* **2000**, *61*, 3135.
- (8) Heine, V. *Nature* **2000**, *403*, 836.

- (9) McMahon, M. I.; Rekihi, S.; Nelmes, R. J. *Phys. Rev. Lett.* **2001**, *87*, 055501.
- (10) McMahon, M. I.; Degtyareva, O.; Nelmes, R. J. *Phys. Rev. Lett.* **2000**, *85*, 4896.
- (11) Needs, R. J.; Martin, R. M.; Nielsen, O. H. *Phys. Rev. B* **1986**, *33*, 3778; *Phys. Rev. B* **1987**, *35*, 9851.
- (12) Chang, K. J.; Cohen, M. L. *Phys. Rev. B* **1986**, *33*, 7371.
- (13) Mattheiss, L. F.; Hamann, D. R.; Weber, W. *Phys. Rev. B* **1986**, *34*, 2190.
- (14) Seifert, K.; Hafner, J.; Furthmüller, J.; Kresse, G. *J. Phys.: Condens. Matter* **1995**, *7*, 3683.
- (15) da Silva, C. R. S.; Wentzcovitch, R. M. *Comput. Mater. Sci.* **1997**, *8*, 219.

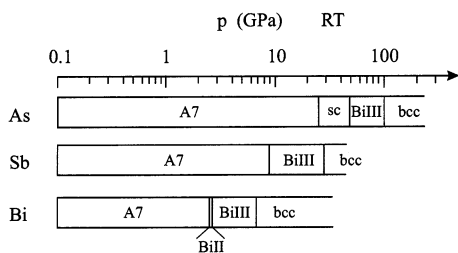


Figure 1. High-pressure structural behavior of the heavier group 15 elements as established by experiment (at room temperature).

pseudopotentials and a plane wave basis set as implemented in the program VASP.¹⁶ Ultrasoft Vanderbilt-type pseudopotentials¹⁷ were employed, and As 4s and 4p, Sb 5s and 5p, and Bi 6s and 6p electrons were treated as valence electrons. We considered the elements in the structure types As (rhombohedral), simple cubic, body centered cubic, Bi-II (monoclinic), and Bi-III (tetragonal). The Bi-III structure corresponds to an incommensurately modulated composite structure. Since conventional electronic structure calculations are based on periodic boundary conditions, an incommensurate structure has to be approximated by a supercell. Details of the structural model are given in the Discussion section. The atomic position parameters and lattice parameters of the structure types As, Bi-II, and Bi-III were relaxed for a set of constant volumes until forces had converged to less than 0.01 eV/Å. In a second step we fitted the E vs V values of all structures to polynomials whose curvature yielded the pressure. After having obtained the pressure, enthalpies H were calculated according to $H(p) = E(p) + pV(p)$. The exchange and correlation energy was assessed by the generalized gradient approximation (GGA).¹⁸ The convergence of the calculations was carefully checked with respect to the plane wave cutoff and the number of k points used in the summation over the Brillouin zone. Concerning the plane wave cutoff, an energy value of 300 eV was chosen for all systems. k points were generated by the Monkhorst–Pack method¹⁹ and sampled on grids of $4 \times 4 \times 4$ (Bi-III type), $15 \times 15 \times 15$ (As and Bi-II types), and $17 \times 17 \times 17$ (sc and bcc types). The integration over the Brillouin zone was performed with a Gaussian smearing of 20 mRy. Total energies were converged to better than 1 meV/atom.

3. High-Pressure Structures of As, Sb, and Bi

The experimentally established high-pressure behavior (at room temperature) of the heavier group 15 elements As, Sb, and Bi is summarized in Figure 1. At ambient pressure the three elements possess the rhombohedral As (A7) structure (space group $R\bar{3}m$) as the ground state structure (Figure 2a).²⁰ The As structure can be described as consisting of layers of six-membered rings in chair conformation. Each atom has three short contacts in the layer and three longer contacts with the atoms of one adjacent layer. This results in a distorted octahedral (3 + 3) coordination. When specifying the As structure with hexagonal axes, the structural parameters are the c/a ratio and the z parameter of the Wyckoff position 6c (0,0, z). Table 1 lists those parameters for the ground states of As, Sb, and Bi, together with the interlayer (d_1) and intralayer (d_2) atomic distances. From As to Bi the c/a ratio of the As structure decreases while the z parameter increases. As a consequence, the interlayer and intralayer distances become less different and the simple cubic

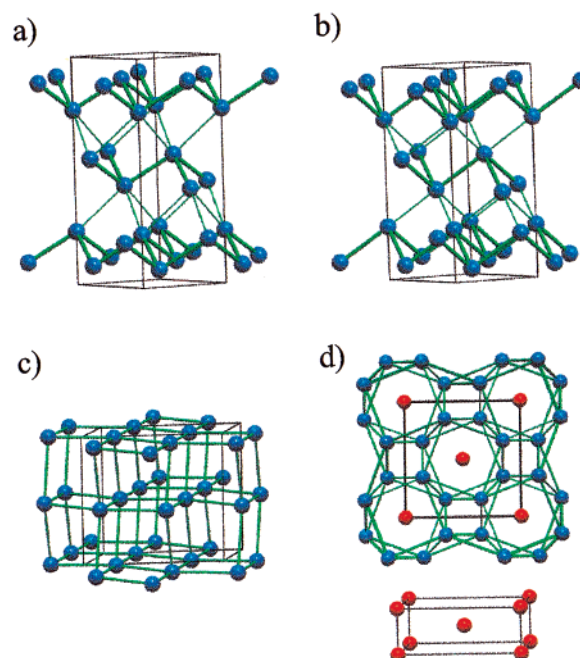


Figure 2. (a) Rhombohedral As (A7) ground state structure of As, Sb, and Bi shown approximately along [110]. Thick green lines denote short interlayer atomic distances and thin green lines the long intralayer ones. In the simple cubic (sc) structure (b) interlayer and intralayer distances have equal length. (c) The monoclinic Bi-II structure shown approximately along [101]. (d) The tetragonal Bi-III structure shown along [001]. Host atoms, blue; guest atoms, red. The guest structure, which is additionally depicted separately below, is incommensurate with the host along [001].

Table 1. Structural Parameters and Atomic Distances in the Heavier Group 15 Elements with the Rhombohedral A7 Structure (Space Group $R\bar{3}m$, Wyckoff Position 6c (0,0, z))²⁰

| | As | Sb | Bi | sc |
|-----------|--------|--------|--------|-------|
| c/a | 2.805 | 2.617 | 2.602 | 2.449 |
| z | 0.2271 | 0.2335 | 0.2341 | 0.25 |
| d_1 [Å] | 2.517 | 2.908 | 3.062 | |
| d_2 [Å] | 3.120 | 3.355 | 3.512 | |
| d_2/d_1 | 1.240 | 1.154 | 1.147 | 1 |

(sc) structure with a perfect octahedral coordination of atoms is approached. In the sc structure c/a attains a value of $\sqrt{6}$ (≈ 2.45) and z becomes 0.25 (Figure 2b).

With pressure As transforms at 25 GPa from the A7 ground state structure to the sc structure (As-II).²¹ For Sb the sc structure is closely approached,²² but the first structural high-pressure transition at 8.6 GPa results in tetragonal Sb-II.²³ Bi transforms already at 2.57 GPa to Bi-II.²⁴ The unique monoclinic structure of Bi-II can be considered as a distorted sc array (Figure 2c).²⁵ Bi-II has a very narrow stability range: at 2.77 GPa the transformation to tetragonal Bi-III takes place. Further, the I-II transition disappears at temperatures around 200 K.²⁶

The tetragonal structure of Bi-III (Figure 2d) has long been uncertain and was only recently identified as a complex incommensurate host–guest structure.¹⁰ The Bi-III structure is

(16) Kresse, G.; Hafner, J. *Phys. Rev. B* **1993**, *47*, RC558. Kresse, G.; Furthmüller, J. *Phys. Rev. B* **1996**, *54*, 11169.
 (17) Vanderbilt, D. *Phys. Rev. B* **1990**, *41*, 7892. Kresse, G.; Hafner, J. *J. Phys.: Condens. Matter* **1994**, *6*, 8245.
 (18) Perdew, J. P.; Wang, Y. *Phys. Rev. B* **1992**, *45*, 13244.
 (19) Monkhorst, H. J.; Pack, J. D. *Phys. Rev. B* **1976**, *13*, 5188.
 (20) Donahue, J. *The Structures of the Elements*; Wiley: New York, 1974.

(21) Beister, H. J.; Strössner, K.; Syassen, K. *Phys. Rev. B* **1990**, *41*, 5535.
 (22) Schiferl, D.; Cromer, D. T.; Jamieson, J. C. *Acta Crystallogr. B* **1981**, *37*, 807.
 (23) Iwasaki, H.; Kikegawa, T. *High Pressure Res.* **1990**, *6*, 121.
 (24) Brugger, R. M.; Bennion, R. B.; Worlton, T. G. *Phys. Lett A* **1967**, *24A*, 714.
 (25) Chen, J. H.; Iwasaki, H.; Kikegawa, T. *High Pressure Res.* **1996**, *15*, 143.
 (26) Young, D. A. *Phase Diagrams of the Elements*; University of California Press: Berkeley, 1991.

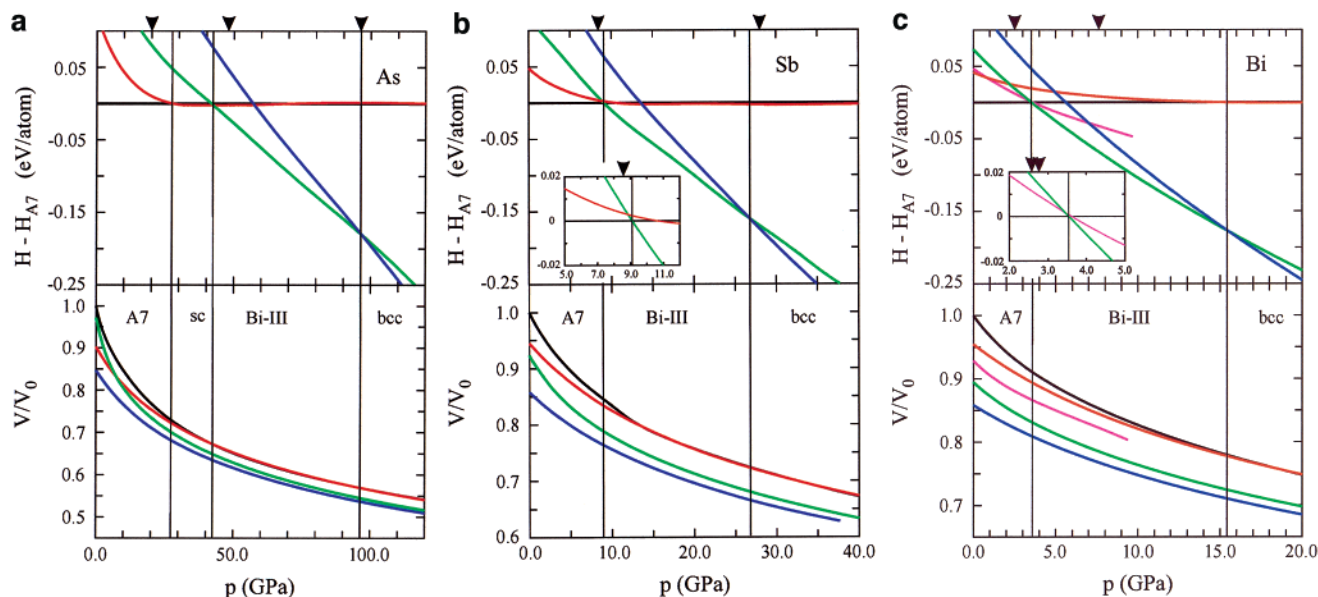


Figure 3. Calculated enthalpy differences (relative to the As (A7) structure) and equations of state for As (a), Sb (b), and Bi (c) as a function of pressure. Red, sc structure; green, Bi-III structure; blue, bcc structure; magenta, Bi-II structure. V_0 is the theoretical ground state volume. The pressure stability ranges of the considered structures are indicated by vertical lines (calculated, zero temperature) and black markers (experimental, room temperature). The insets in (b) and (c) represent closeups of the pressure region of the first structural transition.

also adopted by Sb-II and in a slightly modified way by As-III.¹⁰ The latter phase forms from sc As-II at 48 GPa.²⁷ At high pressures the elements in question transform from the complex Bi-III structure to the body centered cubic (bcc) structure. The bcc structure represents the current end member of the high-pressure structural series of As, Sb, and Bi, and is obtained at pressures of 93,²⁷ 28,²⁸ and 7.7 GPa,²⁹ respectively.

4. Computational Results

Figure 3 summarizes our results concerning the high-pressure behavior of As, Sb, and Bi. It displays calculated enthalpy differences (relative to the As ground state structure) for the elements in the structures under consideration as a function of pressure. Additionally, the corresponding equations of state (EOS; volume as a function of pressure) are shown.

For As we find the following phase transition sequence with increasing pressure: As \rightarrow 28 GPa \rightarrow sc \rightarrow 43 GPa \rightarrow Bi-III \rightarrow 97 GPa \rightarrow bcc. These compare extremely well with the experimental (room temperature) transition pressures of 25 ± 1 ,²¹ 48 ± 11 , and 97 ± 14 GPa,²⁷ respectively. The first structural transition As \rightarrow sc has been the subject of earlier theoretical investigations.^{12,13,15} The transition pressures predicted in these works scattered between 20 and 35 GPa. The calculated volume changes $\Delta V/V_0$ (V_0 is the ground state volume) at the transitions are very small: 0.8% for As \rightarrow sc, 2.5% for sc \rightarrow Bi-III, and 0.8% for Bi-III \rightarrow bcc. This again is in accord with experimental observation. Beister et al. determined the volume change at the first transition to 0.5%.²¹ Greene et al. established the EOS for As up to 122 GPa and found no detectable volume discontinuity for any transition.²⁷ However, the latter authors presented rather sparse EOS data and furthermore erroneously assigned the orthorhombic α -Np structure for As-III.

Turning to Sb, we find the As \rightarrow Bi-III transition at a pressure of 9.1 GPa, which agrees well with the experimental transition pressure of 8.6 GPa.²² The As \rightarrow Bi-III transition occurs just below a hypothetical transformation As \rightarrow sc, for which we calculated a transition pressure of 10.7 GPa. This result coincides with a high-pressure single crystal structure determination of Sb in the As structure, where it was found that Sb initially approaches the sc structure but then levels off and transforms to tetragonal Sb-II.²² For the second high-pressure transition Bi-III \rightarrow bcc, we found a transition pressure of 26.8 GPa, again in good agreement with the experimental value of 28 GPa.²⁸ The calculated volume changes $\Delta V/V_0$ at the transitions are 6.7% for As \rightarrow Bi-III and 2.1% for Bi-III \rightarrow bcc. The value of the first transition corresponds well to the experimental result of McMahon et al., who found a volume change of 6.4% at the Sb-I \rightarrow Sb-II transition.¹⁰ The volume change at the second transition was determined by Aoki et al.²⁸ They estimated the reduction to be about 6%, which is much larger than the calculated value. The deviation is due to the wrong structure assignment for Sb-II by these authors.

Experimentally Bi undergoes the first structural high-pressure transition from the As structure to monoclinic Bi-II at 2.55 GPa.²⁴ This transition is not found in our calculations. Instead, Bi transforms directly from the As structure to Bi-III at a pressure of 3.54 GPa. This is in perfect agreement with the pressure–temperature (p – T) phase diagram of Bi, which reveals that the narrow stability range of Bi-II decreases at lower temperatures and vanishes at about 200 K.²⁶ For the following transition Bi-III \rightarrow bcc, we find a transition pressure of 15.5 GPa. This transition appears to be substantially delayed with respect to the experimentally observed structural change at 7.7 GPa.²⁹ We consider the general accuracy of our calculations to be very high. A possible explanation for the discrepancy is that the Bi-III \rightarrow bcc transition pressure might be highly susceptible to temperature (recall the influence of temperature on the I-II transition) and is shifted to higher pressures at lower temper-

(27) Greene, R. G.; Luo, H.; Ruoff, A. L. *Phys. Rev. B* **1995**, *51*, 597.

(28) Aoki, K.; Fujiwara, S.; Kusakabe, M. *Solid State Commun.* **1983**, *45*, 161.

(29) Aoki, K.; Fujiwara, S.; Kusakabe, M. *J. Phys. Soc. Jpn.* **1982**, *51*, 3826.

atures. Bi differs from the other group 15 elements in having a much more complex p - T phase diagram.²⁶ A look at the p - T phase diagram of Bi reported by Iwasaki et al. supports this explanation.³⁰ When the III-bcc phase line is interpolated to 0 K, a Bi-III \rightarrow bcc transition pressure higher than 12 GPa is obtained. Further, one has also to consider that there might be no direct transition Bi-III \rightarrow bcc at 0 K because of the possible existence of stable low-temperature high-pressure modifications in between. Such modifications have been reported in some older literature.³¹

In conclusion, our calculations were able to reproduce the high-pressure behavior of the heavier group 15 elements As, Sb, and Bi in a highly satisfactory manner. In particular, the close agreement between theoretical and experimental results suggests that our supercell approximation of the incommensurate Bi-III structure describes this complex host-guest arrangement very well. In the next section we discuss in more detail the Bi-III structure and its commensurate model.

5. Discussion

5.1. The Bi-III Structure. The most conspicuous phenomenon in the high-pressure structural sequence of the heavier group 15 elements is the occurrence of a complex incommensurate host-guest structure.¹⁰ The Bi-III structure (cf. Figure 2d) is adopted by Bi-III, by Sb-II, and in a slightly modified way by As-III. The host component is described by the Wyckoff site 8h ($x, x+1/2, 0$) in space group $I4/mcm$ which results in $3^2\cdot 434$ nets stacked in an antiposition orientation along the c direction. Thus, the host structure corresponds to an assembly of rows of square antiprisms which channel linear chains of guest atoms. The guest atom arrangement corresponds to a body centered tetragonal (bct) structure which is incommensurate with the host along the c direction. In As-III the bct guest structure appears to be monoclinically distorted.¹⁰ For Bi-III and Sb-II the ratio between the two c axes, c_H/c_G , is very similar—around 1.31—and interestingly c_H/c_G also varies only very slightly with pressure. The c_H/c_G ratio defines the ratio between host and guest atoms in the Bi-III structure, which is 8:2.620. The proximity of c_H/c_G to the commensurate ratio $4/3 = 1.333$ suggests that the Bi-III structure can be modeled by a commensurate supercell with a trebled host c axis. Thus, the unit cell of the model structure contains 24 host atoms in six $3^2\cdot 434$ nets and 8 bct guest atoms in the channels along $(0,0,z)$ and $(1/2,1/2,z)$. The ratio between host and guest atoms in the model structure is 8:2.667, which implies that its density is slightly higher compared with that of the experimental structure.

We started our investigation with a trial structure consisting of six in antiposition stacked $3^2\cdot 434$ nets (i.e., the host structure) and a perfect bct guest arrangement with an arbitrary origin offset from the host structure. Further, we considered Bi at $V/V_0 = 0.84$ (i.e., close to the lower border of the theoretical stability range). The initial relaxation was performed in space group $P4$ to ensure a maximum degree of structural flexibility within tetragonal symmetry. Most interesting, in the relaxed structure the guest departed the perfect bct arrangement of the starting geometry and we observed a pairing of atoms within the linear chains. A careful inspection of the relaxed parameters of the host and guest atoms showed that the model structure can be

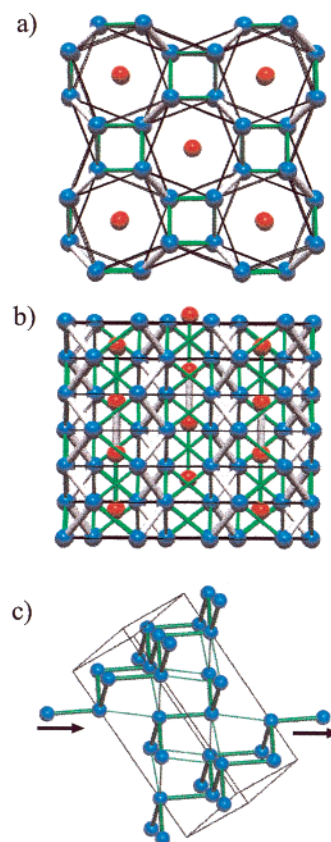


Figure 4. $P4/ncc$ -Bi-III model structure (Bi, $V/V_0 = 0.84$) shown along [001] (a) and [100] (b). Thick gray lines denote the shortest distances within the host (zigzag chains of atoms) and within the guest (pairs of atoms). Medium distances, green lines; long distances (defining the $3^2\cdot 434$ nets), thin black lines. (c) View of the As structure emphasizing the similarity with the Bi-III host structure (zigzag chains) and guest structure (distorted linear chain, marked by arrows).

described with the higher symmetry space group $P4/ncc$. We applied the same procedure for Bi at $V/V_0 = 0.73$ (i.e., close to the upper border of the theoretical stability range) and also for Sb and As at two volumes each and found the same behavior. Finally, we used the model structure with space group symmetry $P4/ncc$ for calculating extended energy-volume curves, from which the results presented in Figure 3 were extracted.

The relaxed $P4/ncc$ model approximating the Bi-III structure (for Bi at $V/V_0 = 0.84$) is shown in Figure 4. In Table 2 we compiled the structural parameters of the $P4/ncc$ -Bi-III model for As, Sb, and Bi at equilibrium volume and at volumes close to the respective lower and upper stability range borders. In Table 3 we compare the corresponding interatomic distances. We first focus on the equilibrium structures (which are only accessible by theory). Each host atom H is sandwiched by two triangles of other host atoms belonging to $3^2\cdot 434$ nets situated above and below the central atom. This yields a trigonal prismatic environment in which, however, the central atom is pronouncedly off-center toward one edge of the trigonal prism. Thus, H-H distances are split into two short and four longer ones. Host atoms connected by the shortest distances form zigzag chains running along the c direction. Additionally, the host atoms are coordinated by two (H2) or three guest atoms (H1), which results in the total coordination numbers of 8 and 9, respectively. In the distorted linear chain guest structure each guest atom G is coordinated by two other guest atoms and (4

(30) Iwasaki, H.; Chen, J. H.; Kikegawa, T. *Rev. Sci. Instrum.* **1995**, *66*, 1388.

(31) Homan, C. G. *J. Phys. Chem. Solids* **1975**, *36*, 1249.

Table 2. Results of the Structure Relaxation of the $P4/ncc$ -Bi-III Model Structure for As, Sb, and Bi, at Three Different Volumes^a

| | Bi | | | Sb | | | As | | |
|---------|-----------------|--------|--------|-----------------|--------|--------|-----------------|--------|--------|
| | V_{eq} | V_2 | V_3 | V_{eq} | V_2 | V_3 | V_{eq} | V_2 | V_3 |
| V/V_0 | 0.898 | 0.844 | 0.735 | 0.910 | 0.785 | 0.691 | 0.970 | 0.662 | 0.529 |
| c/a | 1.491 | 1.487 | 1.485 | 1.457 | 1.469 | 1.480 | 1.363 | 1.460 | 1.488 |
| $H1_x$ | 0.0983 | 0.1004 | 0.0993 | 0.1036 | 0.1037 | 0.1018 | 0.1054 | 0.1061 | 0.1034 |
| $H1_y$ | 0.5840 | 0.5894 | 0.5957 | 0.5713 | 0.5833 | 0.5901 | 0.5473 | 0.5803 | 0.5896 |
| $H1_z$ | 0.0827 | 0.0827 | 0.0834 | 0.0800 | 0.0825 | 0.0833 | 0.0751 | 0.0824 | 0.0834 |
| $H2_x$ | 0.4119 | 0.4072 | 0.4029 | 0.4227 | 0.4106 | 0.4057 | 0.4391 | 0.4118 | 0.4056 |
| $G1_z$ | 0.0414 | 0.0431 | 0.0486 | 0.0413 | 0.0466 | 0.0534 | 0.0348 | 0.0468 | 0.0537 |
| $G2_z$ | 0.3083 | 0.3062 | 0.3060 | 0.3076 | 0.3074 | 0.3100 | 0.3052 | 0.3086 | 0.3099 |

^a V_{eq} , equilibrium volume; space group $P4/ncc$; host atoms H1 at 16g (x,y,z) and H2 at 8f ($x,\bar{x},1/4$); guest atoms G1 and G2 at 4c ($1/4,1/4,z$).

Table 3. Interatomic Distances [\AA] in As, Sb, and Bi in the $P4/ncc$ -Bi-III Model Structure at Three Different Volumes^a

| | Bi | | | Sb | | | As | | |
|---------------|-----------------|-------|-------|-----------------|-------|-------|-----------------|-------|-------|
| | V_{eq} | V_2 | V_3 | V_{eq} | V_2 | V_3 | V_{eq} | V_2 | V_3 |
| V/V_0 | 0.898 | 0.844 | 0.735 | 0.910 | 0.785 | 0.691 | 0.970 | 0.662 | 0.529 |
| | | | | | H1 | | | | |
| H2 | 3.17 | 3.18 | 3.09 | 2.93 | 2.92 | 2.85 | 2.49 | 2.45 | 2.33 |
| H1 | 3.19 | 3.18 | 3.09 | 2.95 | 2.94 | 2.87 | 2.48 | 2.48 | 2.35 |
| G2 | 3.32 | 3.28 | 3.18 | 3.07 | 3.00 | 2.92 | 2.69 | 2.51 | 2.37 |
| H2 | 3.57 | 3.45 | 3.27 | 3.48 | 3.21 | 3.06 | 3.29 | 2.70 | 2.49 |
| $H1 \times 2$ | 3.59 | 3.46 | 3.28 | 3.45 | 3.24 | 3.08 | 3.27 | 2.73 | 2.51 |
| H2 | 3.67 | 3.53 | 3.29 | 3.71 | 3.35 | 3.13 | 3.58 | 2.85 | 2.56 |
| G1 | 3.73 | 3.66 | 3.47 | 3.69 | 3.46 | 3.26 | 3.53 | 2.94 | 2.67 |
| G2 | 3.81 | 3.74 | 3.58 | 3.73 | 3.62 | 3.41 | 3.50 | 3.02 | 2.79 |
| | | | | | H2 | | | | |
| $H1 \times 2$ | 3.17 | 3.16 | 3.09 | 2.93 | 2.92 | 2.85 | 2.49 | 2.45 | 2.33 |
| $G1 \times 2$ | 3.43 | 3.35 | 3.24 | 3.26 | 3.14 | 3.03 | 2.98 | 2.56 | 2.47 |
| $H1 \times 2$ | 3.57 | 3.40 | 3.26 | 3.48 | 3.21 | 3.06 | 3.29 | 2.70 | 2.49 |
| $H1 \times 2$ | 3.67 | 3.46 | 2.29 | 3.71 | 3.35 | 3.13 | 3.58 | 2.85 | 2.55 |
| | | | | | G1 | | | | |
| G2 | 3.10 | 3.06 | 3.01 | 2.93 | 2.87 | 2.81 | 2.51 | 2.40 | 2.31 |
| $H2 \times 4$ | 3.43 | 3.35 | 3.24 | 3.26 | 3.14 | 3.03 | 2.98 | 2.65 | 2.47 |
| G2 | 3.55 | 3.36 | 3.19 | 3.34 | 3.13 | 2.96 | 2.96 | 2.64 | 2.43 |
| $H1 \times 4$ | 3.73 | 3.60 | 3.47 | 3.69 | 3.46 | 3.26 | 3.53 | 2.94 | 2.67 |
| | | | | | G2 | | | | |
| G1 | 3.10 | 3.06 | 3.01 | 2.93 | 2.87 | 2.81 | 2.51 | 2.40 | 2.31 |
| $H1 \times 4$ | 3.32 | 3.26 | 3.18 | 3.08 | 3.00 | 2.92 | 2.69 | 2.51 | 2.37 |
| G1 | 3.55 | 3.36 | 3.19 | 3.34 | 3.13 | 2.96 | 2.96 | 2.64 | 2.43 |
| $H2 \times 4$ | 3.81 | 3.72 | 3.58 | 3.73 | 3.55 | 3.41 | 3.50 | 3.02 | 2.79 |

^a V_{eq} is the equilibrium volume.

+ 4) host atoms. A closer look at the host atom zigzag chains and the guest structure reveals a remarkable relationship to the As ground state structure (Figure 4c). The distorted linear chain arrangement of the $P4/ncc$ -Bi-III guest structure also occurs in the (110) plane of the As structure, with the two interchain distances stunningly similar (cf. Tables 1 and 3). Further, the zigzag chains of the $P4/ncc$ -Bi-III host structure can also be detected in the (012) plane of the As structure. Again, the distances within the chains are almost alike in both structures (cf. Tables 1 and 3), and in addition the bond angle in both kinds of zigzag chains is close to 90° . With pressure the shortest distances in the Bi-III model structure change less and the pairing tendency of the guest atoms weakens (Table 3). The c/a ratio of the Bi-III model structure is only slightly pressure dependent (Table 2). This agrees with the experimental observation that the c_H/a_H and c_H/c_G ratios in Bi-III and Sb-II are almost constant upon pressure variation.¹⁰

With respect to the coordination number of the atoms, the complex Bi-III host–guest structure can be considered as an intermediate structure along the route from the open packed As (and sc) structure toward the densely packed bcc structure.

However, for complex structures with an almost continuous spectrum of atomic distances, it is difficult to define explicit coordination numbers for the constituting atoms. The effective coordination number (econ), as introduced by Hoppe, provides an unambiguous quantification of coordination numbers.³² For the determination of econ, the distance between the central atom and a particular coordinating atom is weighted with an exponential function before summation. Thus, econ allows explicitly the study of the variation of coordination numbers with pressure. This is shown representatively for Sb in Figure 5. Somewhat trivially, in the As structure, atoms approach smoothly the coordination number of 6 as in the sc structure. The coordination number gap between the sc and the bcc structure (econ = 11.3) is filled by the Bi-III structure. With increasing pressure, Bi-III develops into a structure in which the constituting atoms possess an average coordination number of 9. As stated by Heine, there are no simple structures with nine near neighbors, and consequently complex arrangements are observed.⁸ From this purely structural point of view it thus

(32) (a) Hoppe, R. *Angew. Chem., Int. Ed. Engl.* **1970**, *9*, 25. (b) Hoppe, R. Z. *Kristallogr.* **1979**, *150*, 23.

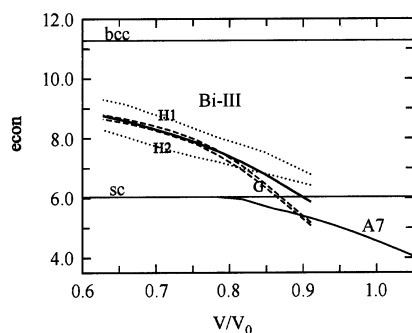


Figure 5. Effective coordination number (econ) for Sb as a function of volume. For the Bi-III structure the econ of the host atoms is drawn with dotted lines and the econ of the guest atoms with broken lines. The thick solid lines represent the average econ of the atoms in the Bi-III structure.

seems natural to observe complex intermediate structures in the high-pressure structural sequence of, e.g., group 14 or 15 elements with low coordination number ground state structures. We return to this point in the following section where we discuss electronic structure trends.

The energy difference between the commensurate $P4/ncc$ model structure and the experimental structure can be considered as extremely low (on the order of millielectronvolts per atom), since the model structure fits perfectly the experimental transition pressures. We recall that the model structure differs from the experimental structure by the slightly higher density of the guest component and the distorted linear chain arrangement of the guest atoms. However, a very recently performed full four-dimensional refinement of a Bi-III single crystal revealed further modulations of the host and guest structures.³³ Intriguingly, the additional modulation of the guest structure agrees with the pairing tendency of atoms within the linear chains as found in the supercell model. This pairing is certainly associated with the tendency of the heavier group 15 elements to form homonuclear covalent bonds (in the equilibrium Bi-III model structure the short distance within the linear chains corresponds for each element to a single bonded pair; cf Tables 1 and 3). Then, in a speculative way, incommensurate modulations could be a consequence of optimizing host–guest interactions for a guest component which at the same time tries to realize an individual structure (i.e., pairs of atoms). The valence charge distribution in the guest component of the Bi-III model structure, which is shown in Figure 6 for Sb, supports the idea of covalently bonded pairs of atoms within the chains of guest atoms.³⁴ After having discussed in detail the high-pressure crystal structural trends of the heavier group 15 elements, we turn in the next section of this paper to the accompanying electronic structure trends.

5.2. Electronic Structure Changes under Pressure. We have computed the electronic density of states (DOS) of As, Sb, and Bi in the ground state and high-pressure structures, and the curves obtained have been assembled in Figure 7. Figure 7a compares the electronic structure of the group 15 elements

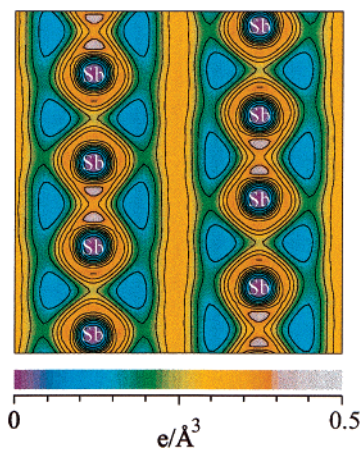


Figure 6. Valence charge distribution in the guest component of Sb-II ($V/V_0 = 0.72$). The charge distribution is presented in a range between 0.0 and $0.5 \text{ e}/\text{\AA}^3$ with contours $n \times 0.05 \text{ e}/\text{\AA}^3$.

in the As structure at the ground state volume V/V_0 . Most conspicuous is the characteristic splitting of the DOS into four parts: s–s bonding, s–s antibonding, p–p bonding and p–p antibonding. The Fermi level is located between the p–p bonding and antibonding bands in a deep pseudogap with a very low value of density of states. This is in agreement with the semimetallic behavior of those elements.

Figure 7b compares the DOS of the three elements in the As structure at a volume close to the transition to the respective first high-pressure structures. With pressure, bandwidths and the density of states at the Fermi level increase. These effects, however, are hardly recognizable for Bi due to the low As \rightarrow Bi-II transition pressure. The materials remain pronounced semimetallic. Figure 7c shows the DOS for sc As, (hypothetical) sc Sb, and Bi-II at a volume slightly above the respective transition pressures. The overall shape of the DOS curves is very similar to that obtained in the compressed As ground state structure (cf. Figure 7b; note that in the monatomic sc structure s- and p-based bands are not split). However, the density of states at the Fermi level is drastically increased and the deep pseudogap separating p–p bonding from antibonding states has changed into a shallow, although marked, well. This emphasizes the first-order character of the As \rightarrow sc (semimetal–metal) transition, despite the accompanying small structural changes. For Bi, the As \rightarrow Bi-II transition also corresponds to a semimetal–metal transition. Figure 7d shows the DOS of the elements in the host–guest Bi-III structure at a volume approximately corresponding to the center of the respective pressure stability ranges. Apart from their spikey feature, which is due to the complexity of the Bi-III structure, the overall shape of the curves is reminiscent of sc As, sc Sb, and Bi-II, respectively.³⁴ Importantly, the Fermi level is still located at a recognizable valley in the p bands. The persistence of the p band bonding–antibonding splitting in the Bi-III structure indicates the presence of a still significant covalent bonding contribution in the high-pressure phases As-III, Sb-II, and Bi-III. This is also reflected in the valence charge distribution (cf. Figure 6). Finally, Figure 7e displays the DOS of As, Sb, and Bi in the bcc structure at a volume close to the Bi-III \rightarrow bcc transition pressure. In the densely packed bcc structure, the Fermi level is no longer situated in a well. For bcc As (highest

(33) McMahon, M. I.; Degtyareva, O.; Nelmes, R. J.; van Smaalen, S.; Palatinus, L. Manuscript in preparation.

(34) Interestingly, the analysis of the electronic structure of the Bi-III model structure of As, Sb, and Bi shows a very similar distribution of the density of states when projected on the host and guest atom sites. This means that there is no significant electronic structure difference between the host and guest component within the Bi-III structure. In particular, the intuitive picture of differently charged host and guest atoms is not supported by our calculations.

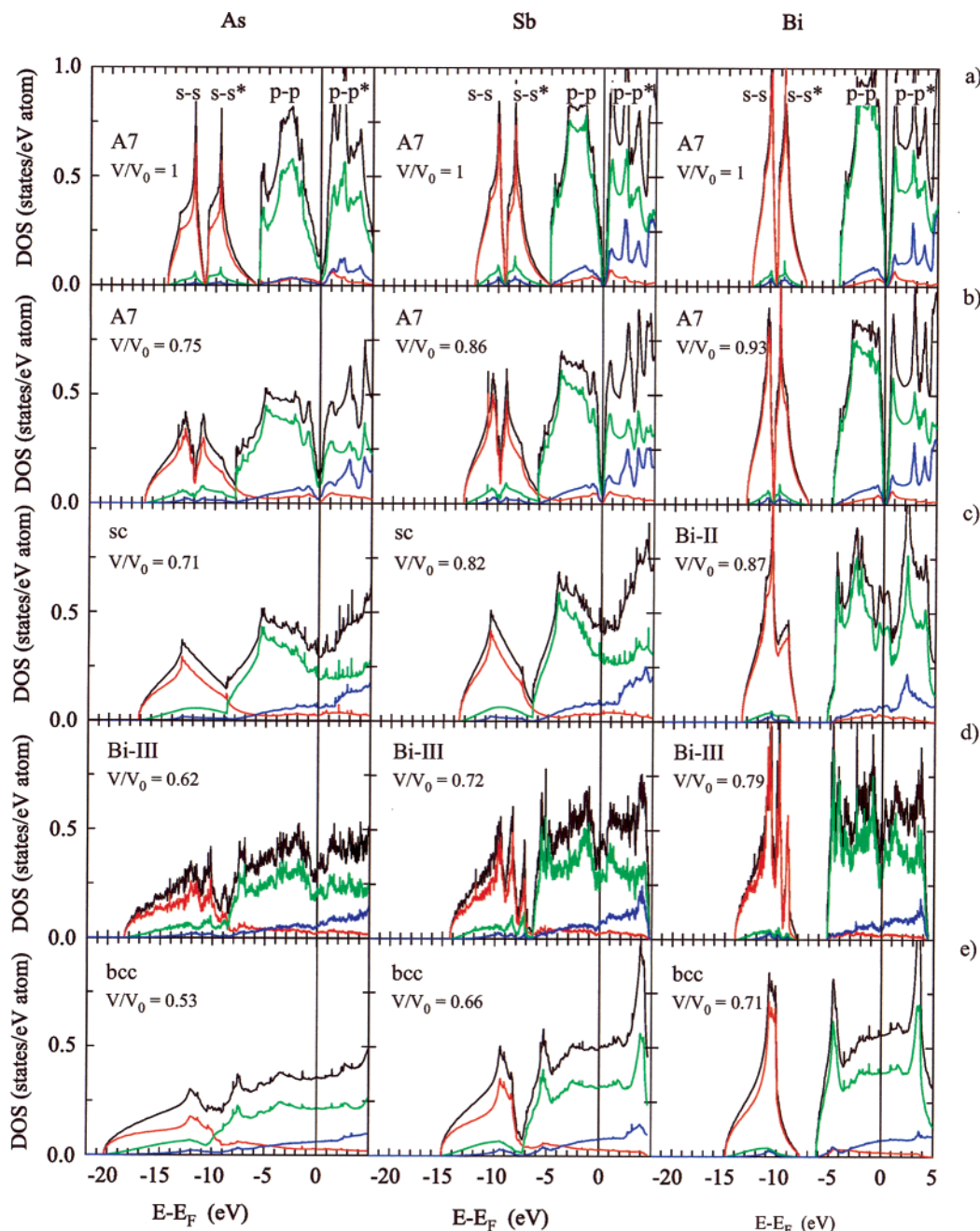


Figure 7. Density of states (DOS) of As, Sb, and Bi in the ground state and high-pressure structures. Black, total DOS; red, s-projected DOS; green, p-projected DOS; blue, d-projected DOS.

compression) the DOS attains an approximately parabolical nearly-free-electron distribution.

We may summarize the general trend in the electronic structure of the heavier group 15 elements under compression as follows: Due to the atomic electron configuration s^2p^3 the Fermi level is located at the center of the p-based bands. In the ground state structure these bands exhibit a pronounced bonding–antibonding splitting, which gradually decreases under compression and finally disappears in the densely packed bcc structure. In that respect, the Bi-III structure again takes an intermediate position between the sc and bcc structures. The rather smooth changes in the electronic structures of As, Sb, and Bi indicate that the valence state of the elements is not changed with pressure. This is in contrast to alkali metal and

alkaline earth metals, where s–p (Li) or s–d transitions (Cs, Ca, Sr, Ba) lead to dramatic electronic structure changes.^{1,35}

To understand high-pressure structural transitions, it is advantageous to divide the total energy into the band energy E^{band} , which represents the sum over the occupied one-electron states (as presented in Figure 7), and a part containing the remaining contributions, of which the electrostatic (Madelung) energy that includes the repulsion of the positively charged ions is the most significant. E^{band} favors the formation of open packed structures in which the atoms are closer to each other and thus covalent bonding can be realized. The electrostatic contributions (summarized as E^{Mad}) display an antagonistic behavior with the

(35) (a) McMahan, A. K. *Phys. Rev. B* **1984**, *29*, 5982. (b) Ahuja, R.; Eriksson, O.; Wills, J. M.; Johansson, B. *Phys. Rev. Lett.* **1995**, *75*, 3473.

tendency to stabilize high-symmetry densely packed structures. In that respect the bcc structure is the most favorable structure of all dense packings (bcc, fcc, hcp), since it has the highest Madelung constant.³⁶ Clearly, for the group 15 elements As, Sb, and Bi, E^{band} determines the As ground state structure. The two total energy contributions E^{band} and E^{Mad} behave differently when the volume V/V_0 is varied. Due to its largely Coulombic nature, E^{Mad} varies approximately as $(1/(V/V_0))^{1/3}$ whereas E^{band} alters in a more complicated way, dependent on how the bandwidths of the different valence bands change with volume. Usually, the E^{Mad} contribution increases relative to E^{band} under compression and densely packed structures are obtained as high-pressure modifications.

How does E^{band} for the heavier group 15 elements evolve with pressure? To answer this question, we analyze the trend in the number of occupied s, p, and d states (N_l). In particular, we calculated the ratios $X_l = N_l/N_{\text{tot}}$ (N_{tot} being the total number of occupied states) for As, Sb, and Bi in the different structures at different volumes (Figure 8). Generally, in any atom arrangement of group 15 elements with an electron configuration s^2p^3 the resulting electronic structure will possess a large number of occupied s-s antibonding states. Thus, for these elements optimizing E^{band} is equivalent to diminishing the number of s-s antibonding states below the Fermi level while keeping favorable p-p bonding. Or, to put it simply, E^{band} will be lowest for that structure which expresses the lowest value of X_s . For the ground state volume and at moderate compressions, the As structure displays the lowest values of X_s among all considered structures for all elements. It was recently shown by Seo and Hoffmann that this is a result of s-p mixing: Lone pair formation at each site is equivalent to a situation in the band structure where strongly s-s antibonding states are partly raised above the Fermi level, and in exchange, p-p nonbonding or weakly antibonding states are lowered below the Fermi level.³⁷ At higher compressions the admixture of empty d states becomes important, and this stabilizes the sc structure. The sc structure attains the lowest values of X_s for all elements at lower volumes. The evolution of s-d hybridization is nicely seen in the trends displayed by the X_s and X_d curves. X_s and X_d vary in a correlated way with pressure, the former decreasing and the latter increasing. X_p remains more or less constant over the whole range of compression. Importantly, for the heavier group 15 elements s-d mixing increases smoothly with pressure and remains at a rather low level. Therefore, the admixture of d states does not lead to a change in the valence state of As, Sb, or Bi. This might be different for the lighter congener P as is indicated in the very large pressure stability range of the sc-P structure (around 100 GPa)³⁸ compared to sc-As (23 GPa).²⁷ Figure 8 also shows clearly that the stabilizing mechanism of s-p or s-d mixing affects especially the more open packed structures (As or sc) and additionally diminishes from As to Bi. Interestingly, the intermediate position of the Bi-III structure between the open packed As and sc structures and densely packed bcc becomes once more apparent. At low compressions this structure yields X_l values close to that of the open packed structures, and with increasing pressure the X_l values of the bcc structure are approached.

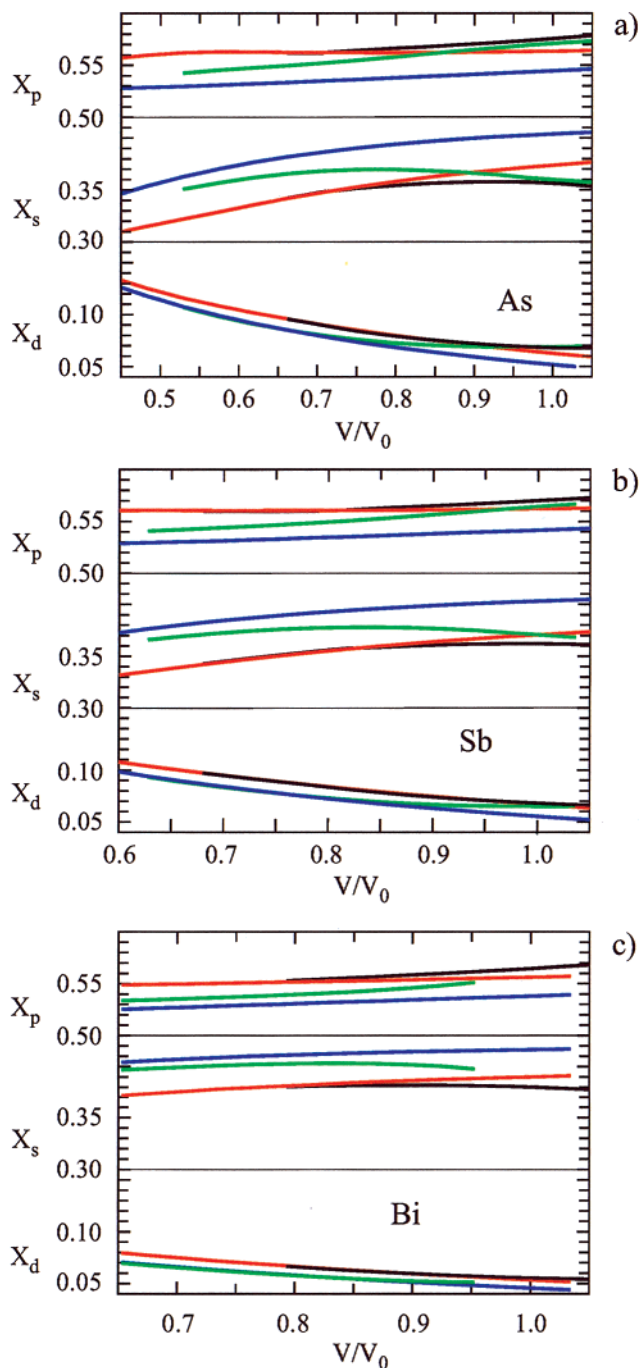


Figure 8. Ratios $X_l = N_l/N_{\text{tot}}$ for As (a), Sb (b), and Bi (c) as a function of volume. N_l ($l = s, p, d$) is the number of occupied s, p, and d states; N_{tot} is the total number of occupied states. Black, As structure; red, sc structure; green, Bi-III structure; blue, bcc structure.

In conclusion, the high-pressure structural sequence of the heavier group 15 elements can be understood as follows: At the ground state volume and moderate compressions E^{band} governs structural stability and the open packed structures As and sc are realized for electronic reasons. The former is stabilized by s-p mixing the latter by s-d mixing. With increasing pressure the significance of E^{band} to structural stability gradually lowers and that of E^{Mad} increases. The complex Bi-III intermediate pressure structure is the consequence of a delicate interplay between E^{band} and E^{Mad} , i.e., both important parts of the total energy account equally for structural stability. This is

(36) Pettifor, D. G. *Bonding and Structure of Molecules and Solids*; Clarendon Press: Oxford, 1995.

(37) Seo, D.-K.; Hoffmann, R. J. *Solid State Chem.* **1999**, *147*, 26.

(38) Akahama, Y.; Kobayashi, M.; Kawamura, H. *Phys. Rev. B* **1999**, *59*, 8520.

expressed in the maintenance of a p band bonding–antibonding splitting in the density of states and the realization of high average coordination numbers at the same time. Finally, at high pressures E^{Mad} governs structural stability and the densely packed bcc structure is formed for electrostatic reasons.

6. Conclusions

The high-pressure structural sequence of the heavier group 15 elements is distinguished by the occurrence of a complex incommensurately modulated host–guest structure. This is the Bi-III structure which is adopted by the phases Sb-II, Bi-III, and, in a slightly modified way, As-III.¹⁰ Host–guest structures formed by elements are most surprising, but may happen more frequently than previously supposed, since this phenomenon is also found in high-pressure modifications of alkali and alkaline earth metals.^{6,7,9} We performed a comparative theoretical study of the high-pressure behavior of the heavier group 15 elements As, Sb, and Bi. The Bi-III structure was approximated by a supercell, which reproduced the experimentally established transition pressures extremely well. The group 15 element phases with the Bi-III structure emerge from either the As ground state structure (for Sb and Bi) or from the sc structure (for As) and transform further to the densely packed bcc structure at high pressures. Thus, the intermediate pressure Bi-III structure is the most complex in the high-pressure structural sequence of these elements. The occurrence of complex intermediate pressure structures seems natural for group 15 elements when considering a steady increase in coordination number with pressure. The effective coordination number (e_{con})³² increases from around 4 in the As structure at the ground state volume to around 6 when the sc structure is approached. In the complex Bi-III

structure the average coordination number changes from 7 to 9 with increasing pressure. Finally, in the bcc structure e_{con} attains a value slightly above 11. In this respect, the Bi-III structure fills the coordination number gap between the open packed structures As and sc and the densely packed bcc structure.

This regular behavior requires that the band energy contribution to the total energy varies smoothly with pressure, which is generally the case when the valence state of the elements is maintained under compression. For the heavier group 15 elements we indeed find a smooth variation of the electronic structure under compression, with an increasing admixture of d states (s–d hybridization) in the occupied states of the high-pressure structures. This s–d mixing remains at a low level and does not introduce an altered valence state. A different situation is encountered for the alkaline earth metals Sr and Ba, which also adopt a host–guest high-pressure structure. For these elements the complex structure evolves from a denser packed structure; i.e., the pressure–coordination rule is violated. It is well-known that the band energy of the heavier alkaline earth metals varies discontinuously with pressure because of the s–d transition of their valence states.³⁵ Thus, for these elements the formation of a complex intermediate pressure structure is due to electronic reasons,³⁹ whereas for the group 15 elements it is rather for electrostatic reasons.

Acknowledgment. This work was supported by the Carl Trygger Foundation.

JA020832S

(39) Reed, S. K.; Ackland, G. J. *Phys. Rev. Lett.* **2000**, *84*, 5580.